40th AIAA/ASME/SAE/ASEE Joint Propulsion Conference and Exhibit
11-14 July 2004, Fort Lauderdale, Florida

AIAA 2004-3585

Analytical Study on Flight Performance of an Air-Breathing RP Laser Launcher

Hiroshi KATSURAYAMA,[*] Masato USHIO,[*] Kimiya KOMURASAKI,[†] and Yoshihiro ARAKAWA[‡]
The University of Tokyo
7-3-1 Hongo,Bunkyo-ku, Tokyo 113-8656, JAPAN

Keywords: Laser Propulsion, Flight analysis, Launch cost

Abstract

An Air-breathing RP Laser Launcher has been proposed as the alternative to conventional chemical launch systems. This paper analytically examines the feasibility of SSTO system powered by RP lasers. The trajectory from the ground to the geosynchronous orbit is computed and the launch cost including laser-base development is estimated. The engine performance is evaluated by a cycle analysis and validated by CFD computations. The results show that the beam power of 1.6MW per unit initial vehicle mass is optimum to reach a geo-synchronous transfer orbit, and 4,000 launches are necessary to redeem the cost for laser transmitter.

INTRODUCTION

Schematic of a vehicle boosted by laser beams is shown in Fig. 1. When laser beam is transmitted from the ground and focused by the parabola nozzle, breakdown occurs near the focus, and plasma is formed. The plasma absorbs the following part of beamed energy and expands outward generating shock waves. The shock waves reflect on the nozzle surface, generating impulsive thrust. Because the energy is provided from the ground and the atmospheric air is utilized as a propellant, neither energy source nor propellant is loaded on the vehicle. Thereby, this type of launcher is expected to achieve a high payload ratio and a low launch cost.

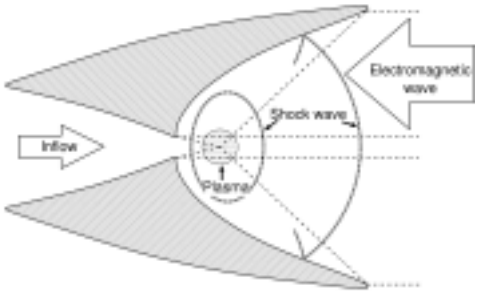

Fig. 1 Vehicle boosted by RP laser beams.

Although many experimental and analytical studies have been carried out on beaming propulsion,[1-4] feasibility studies of the system are quite few. We propose a launch system from the ground to a Geosynchronous Transfer Orbit (GTO) by RP laser propulsion. In the initial stage of launch, the vehicle closes the inlet and takes the air from the rear. This flight mode is called “pulsejet mode”. When ram-compression becomes available as vehicle velocity increases, the inlet is opened and the flight mode is switched to “ramjet mode”. When the vehicle cannot breathe sufficient air at high altitudes, the flight mode is switched to “rocket mode.” Through these three modes, the vehicle is accelerated to reach the orbital velocity.

BEAM TRANSMISSION

High power and large-scale lasers such as chemical, free electron and solid-state lasers are under development for directed energy systems, though there are obstacles in scaling up of a laser oscillator: In general, with the increase in power and size of a laser oscillator, it becomes quite expensive and difficult to oscillate in a single transverse mode to produce optimum beam collimation.

A phased laser array as shown in Fig. 2 is one of the solutions.[5] It will reduce the development cost drastically. However, spatial coherence of arrayed transmitters would be degraded because the profile becomes inevitably a cluster of multiple beams without any overlapping between each other. Therefore, it would be important to know the combined diffraction patterns and their dependency on geometric parameters of the array.

* Graduate student, Department of Aeronautics and Astronautics, Student member AIAA.
† Associate Professor, Department of Advanced Energy, Member AIAA.
‡ Professor, Department of Aeronautics and Astronautics, Member AIAA.

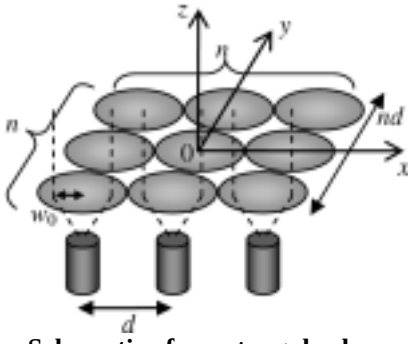

Fig. 2 Schematic of a rectangular laser array.

Computed far-field diffraction patterns were shown in Fig.3. $z_F \equiv (nd)^2/\lambda$ is the boundary distance between Fresnel and Fraunhofer regions. Because its profile on the transmitter is almost flat, far-field profiles tend to consist of a main lobe and several side lobes. Since it would be disadvantageous to collect the power in side lobes from the viewpoint of receiver size, we assume to use only a main lobe for energy transmission.

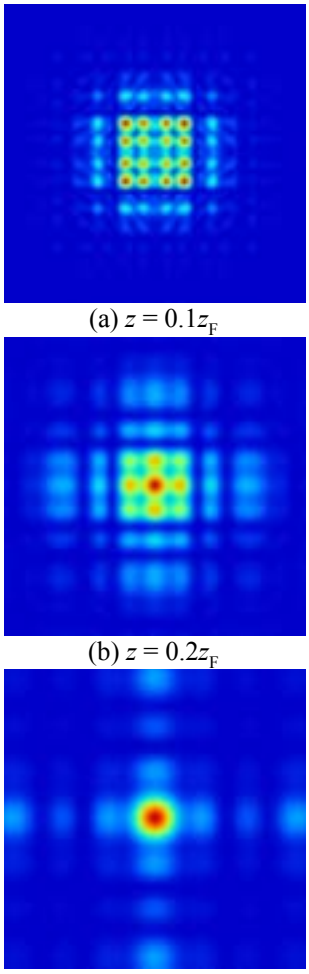

(a) $z = 0.1z_F$

(b) $z = 0.2z_F$

(c) $z = 0.4z_F$

Fig. 3 Calculated Beam Patterns[5]

The fractional energy contained in the main lobe is expressed in terms of the main lobe energy efficiency, η_{ML}. Computed η_{ML} is plotted in Fig.4.

η_{ML} is increased with the aperture fill factor $f \equiv 2w_0/d$. This relationship is valid for array number n at $z > 2z_F$, and can be fitted using a following polynomial function as

$$\eta_{ML} = -0.241f + 2.54f^2 - 1.58f^3. \quad (1)$$

η_{ML} of 0.72 will be attainable with $f \approx 1$.

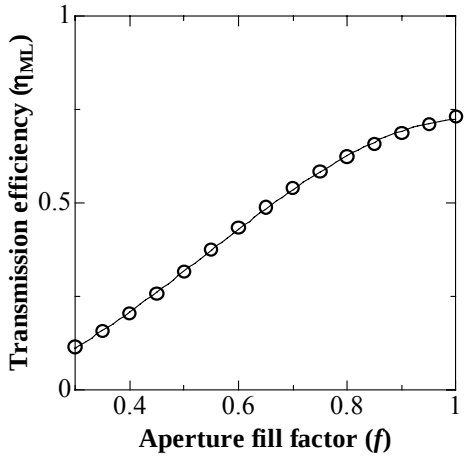

Fig.4 Fractional Transmission Energy and Aperture fill Factor[5]

PROPOSED TRAJECTORY TO THE GEOSYNCHRONOUS ORBIT

We propose a vertical launch to minimize the development cost of the laser base. The laser transmitter can be fixed on the base because it is free from tracking and pointing. The beam degradiation due to the atmospheric turbulence is also minimized. Figure 5 shows the prposed trajectory: The vehicle is boosted by beaming propulsion to reach the orbit beyond the GEO. At the apogee point, the vehicle is kicked to a GTO by an on-board motor and decelarated at the perigee point as well.

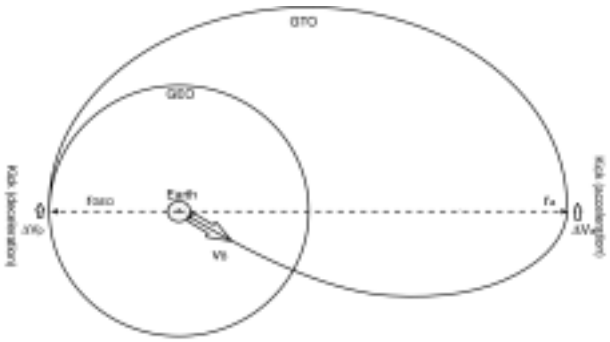

Fig. 5 Proposed trajectory to GEO

Figure 6 shows the nessesary velocity increment by an on-board motor assuming the Hohmann transfer. If the vheicle is boosted to have the velocity of 10.85km/s, nessesary velocity increment by the on-board motor is only 2km/s,

which will be achieved by electric propulsion.

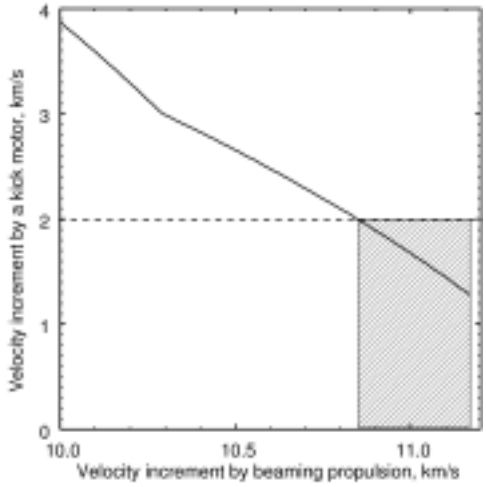

Fig. 6 Required velocity increment from GTO to GEO. Electric propulsion will serve as an upper-stage engine.

THRUST PERFORMANCE

Thrust performace duirng the pulsejet mode has be evaluated by means of ground tests. Schematic of our thrust measurement system[6,7] is shown in Fig. 7. The focus of optics was set in the vicinity of the apex of nozzle cone, and the impulse imparted to the cone I was measured using a ballistic pendulum. The pendulum displacement was measured using a laser distance measurement sensor. The cone angle α, nozzle length $\tilde{r}_n$ and laser energy E_i were varied. The inner wall of nozzle was made of aluminum, and each cone was encased in a cylinder so that the thrust force was not exerted on the outer surface of the nozzle.

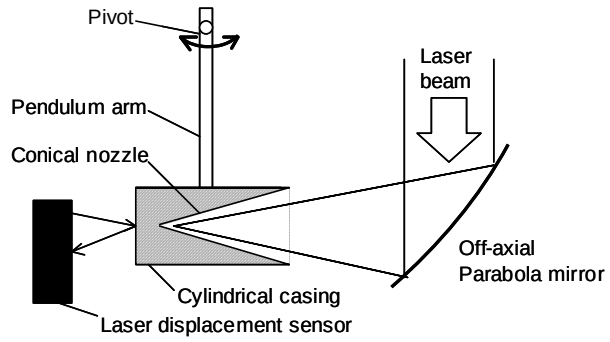

Fig. 7 Impulsive thrust measurement system using a 10J/pulse CO2 Laser

The relation between the momentum coupling coefficient $C_m(\equiv I/E_i)$ and the nozzle length is shown in Fig.8. The nozzle scaling $\tilde{r}_n$ is defined as $\tilde{r}_n = R_n / R^*$. R_n is an actual nozzle length and R^* is a characteristic radius of shock wave defined as,

$$R^* = \left(\frac{E_i / \sin^2(\alpha_d/2)}{p_a} \right)^{\frac{1}{3}} \qquad (2)$$

p_a is an ambient pressure. R^* is a measure of the strength of explosion, and this is equivalent to the radius of the shock wave R_s when the pressure at the shock front decayed mostly to p_a. C_m was found to take maximum value of about 350Ns/MJ at $\tilde{r}_n = 0.3$.

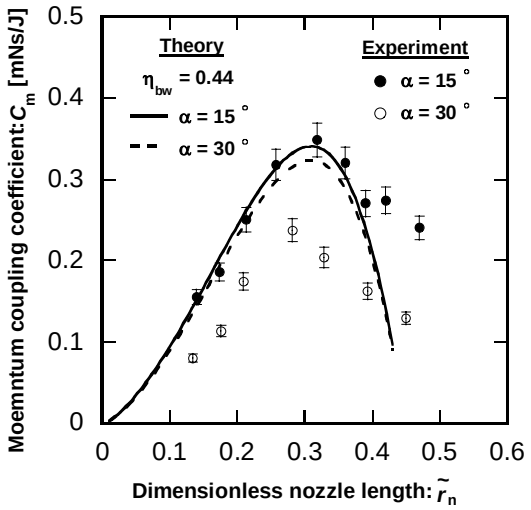

Fig. 8 Measured C_m and dimensionless nozzle length[6,7]

FLIGHT ANALYSIS OF RP LASER LAUNCH SYSTEM

Analysis method

Thrust during the pulsejet mode can be estimated using the measured data of C_m.[1] In the ramjet mode, the airflows inside the vehicle must be considered. Thrust was calculated by an engine cycle analysis similar to those for scramjet engines. The Humphrey cycle as indicated in Figs. 9 and 10 is assumed. Area ratios to vehicle cross-sections S at Positions #0 ~ #4 in Fig. 9 are listed in Table 1. An effective inlet area A_0 is defined as

$$A_0 = S \int_{S_{inlet}} \rho v \cdot dS \Big/ \int_S \rho v \cdot dS \qquad (3)$$

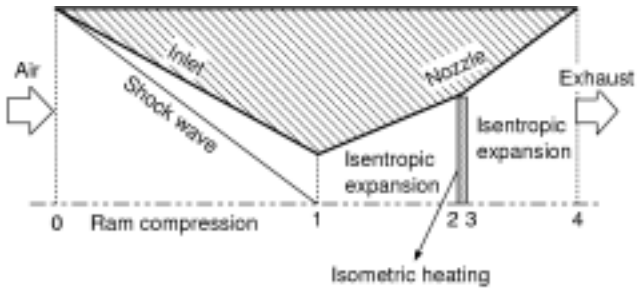

Fig.9 Laser boosted ramjet engine cycle.

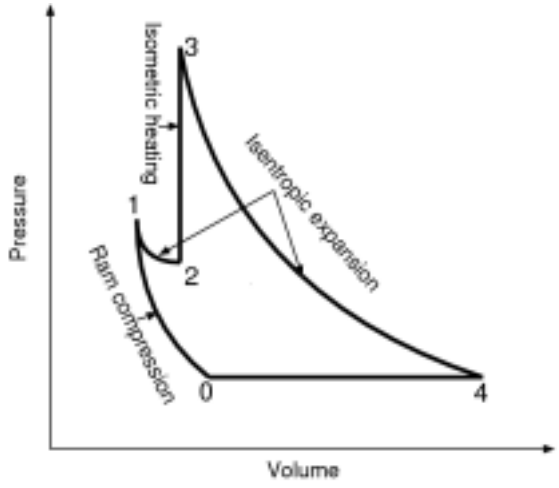

Fig. 10 Humphrey cycle with additional isentropic expansion #1 → #2.

Table 1 Area ratios of assumed vehicle configuration.

S	A_0/S	A_1/S	$A_2/S = A_3/S$	A_4/S
1m^2	0.6	0.38	0.75	1

From Position #0 to #1, air is ram-compressed as

$$\frac{p_{t1}}{p_{t0}} = \left[1 + (1-\eta_d)\frac{\gamma-1}{2}M_0^2\right]^{-\frac{\gamma}{\gamma-1}} \quad (4)$$

where t designates stagnation point, η_d and γ were assumed as 0.97 and 1.4, respectively., The air is isentropically expanded from #1 to #2 and isometrically heated from #2 to #3. Physical properties at #3 were calculated as

$$\rho_3 = \rho_2, u_3 = u_2, T_3 = T_2 + \frac{\eta_B \eta_{ML} \eta_T P_L}{C_p \dot{m}_p},$$
$$p_3 = \rho_3 R T_3,$$
$$M_3 = u_3/\sqrt{\gamma R T_3} \quad (5)$$

where η_B is the fraction of laser energy that is converted to blast wave energy and set to 40%.[8] Finally, the air was again isentropically expanded from #3 to #4, and thrust was calculated as the following:

$$F = \dot{m}_p(u_4 - u_0) + A_4(p_4 - p_0) \quad (6)$$

The mass flow rate taken from the inlet decreases with the altitude due to the decrease in air density. The flight mode is switched to the rocket mode just before thermal choking occurs. The inlet is closed and hydrogen propellant is injected between #1 and #2. The propellant is laser-heated from #2 to #3 and the flow is assumed to choke thermally at #3. Since the energy of flow before heating is negligibly small compared to the laser energy input, the following relations are derived from the energy conservation law and the equation of state:

$$T_3 = \frac{\eta_B P_L}{\dot{m}_p}\left[\frac{2}{C_p(\gamma+1)}\right], \quad (7)$$

$$p_3 = \frac{\dot{m}_p}{A_3}\sqrt{\frac{RT_3}{\gamma}}. \quad (8)$$

From #3 to #4, isentropic expansion was assumed.

Vertical launch trajectories are calculated by solving the following equation of motion by the 4th order Runge-Kutta scheme:

$$m_v \frac{dU}{dt} = F - \frac{1}{2}\rho_\infty U^2 S C_d - m_v g \quad (9)$$

where m_v and U is the vehicle mass and flight speed, respectively. Herein, flight conditions were decided by tracing the trajectory. Drag coefficient C_d is a function of M.[9]

Validation by CFD analysis

In order to validate the results of engine cycle analysis, computed C_m of the ramjet mode was compared with our CFD computations.[4] Figure 11 shows the pressure contour and thrust at 20μs after an explosion. The result is shown in Table 2. The performance at high Mach number is somewhat under-estimated in the engine cycle analysis.

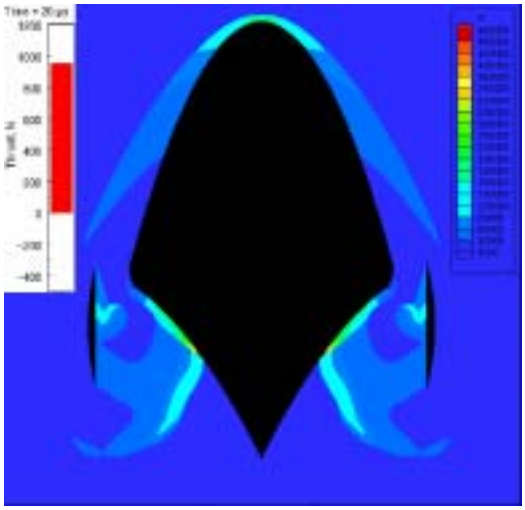

Fig. 11 Pressure contours at *t*=20μs at *H*=20km *M*=5.

Table 2 Comparison of C_m between CFD and Engine Cycle Analysis.[4]

H, km	M	C_m(CFD),Ns/MJ	C_m(ECA),Ns/MJ
20	5	66.0	58.4
30	8	41.0	22.7

Flight Trajectory and Payload Ratio

A payload ratio λ is estimated using the results of engine cycle analysis, which is a conservative estimation.

$$\lambda = \frac{m_{v0} - \frac{\int \dot{m}_p dt}{1-\varepsilon}}{m_{v0}} \quad (10)$$

The structure weight ratio ε is assumed as 0.1 because of its simple structure. The final vehicle is set at 10.85 km/s.

Figures 12 and 13 show the boosting trajectories and payload ratios for several beam power. λ decreases with the beam power per initial vehicle mass P_L/m_{v0}. The period of the ramjet mode also decreases with P_L/m_{v0}, and the ramjet mode is unavailable at $P_L/m_{v0} < 1.5$MW/kg. Beam transmission of up to 300-400km and duration of 60-160s are requested.

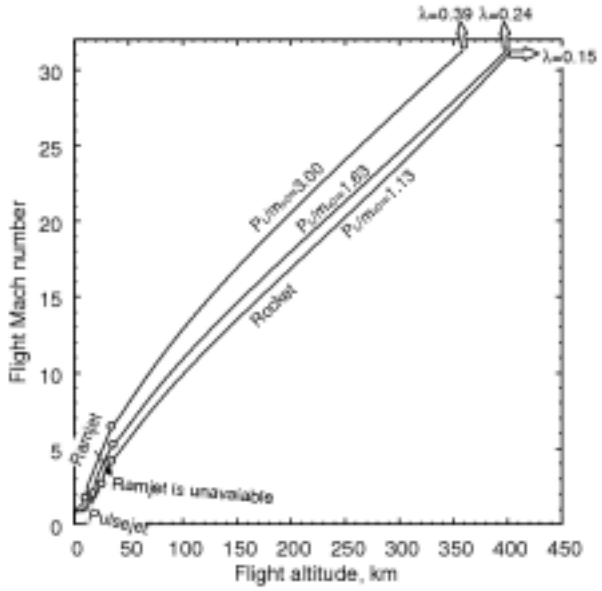

Fig. 12 Flight Mach number and flight altitude

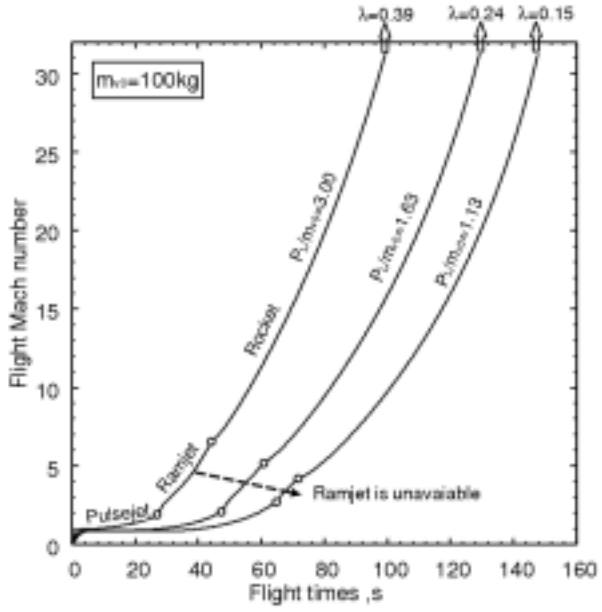

Fig. 13 Flight Mach number vs. flight time

Figure 14 shows the vehicle acceleration for the case of P_L/m_{v0}=1.6 MW/kg. The vehicle is transiently almost stationary in the pulsejet period due to the equilibrium between the aerodynamic drag and the thrust. The acceleration impulsively increases at the mode starting of the pulsejet and ramjet. The acceleration gradually increases with a decrease in the fuel during the rocket mode. The maximum acceleration is about 27*g*.

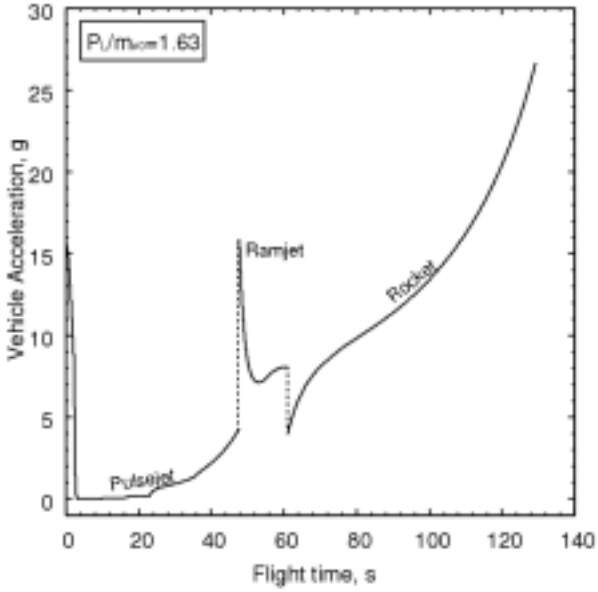

Fig. 14 Vehicle acceleration history.

Figure 18 shows payload mass per unit beam power vs. P_L/m_{v0}. The optimum payload mass per unit beam power is 0.148 kg/MW at P_L/m_{v0} = 1.6 MW/kg. In other words, this is the optimum condition minimizing the development cost of laser base facilities.

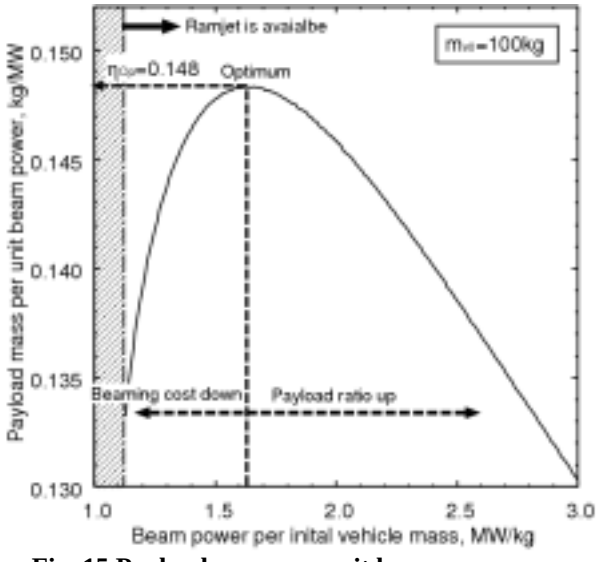

Fig. 15 Payload mass per unit beam power

LAUNCH COST

The costs for laser base facilities, electricity and vehicle fabrication are considered. Table 3 shows the expected costs for beam transmitters. The other costs are tablated in Table 4.

Table 3 Cost for beam transmitters

Transmitter	Cost, $/W	Efficiency
Laser	10	30%
Microwave	0.1	90%

Table 4 Other costs

Electricity	0.06 $/kWh
Vehicle fabrication	4,000 $/kg

Figure 16 shows the relationship between the launch cost and launch count. The cost for beam transmitters is predominant when the lauch count is few. The launch cost decreases with the launch count, and the beam transmitter cost will be redeemed at 4,000 launches compared with that for chemical launchers.

For example, for the construction of a 100-ton space solar power satellite in GEO, chemical launchers can deliver it with 50 launches. Instead, laser beaming propulsion with the capability of 10kg payload/launch can deliver it with 10,000 launches and the cost is going to be half of chemical propulsion. A 100MW-output laser facility is required.

If microwave beaming launcher[10,11] with the capability of 100kg payload/launch is available, 1,000 launches are necessary and cost is almost one-tenth of chemical rockets' cost. A 1GW-outpot microwave facility is required.

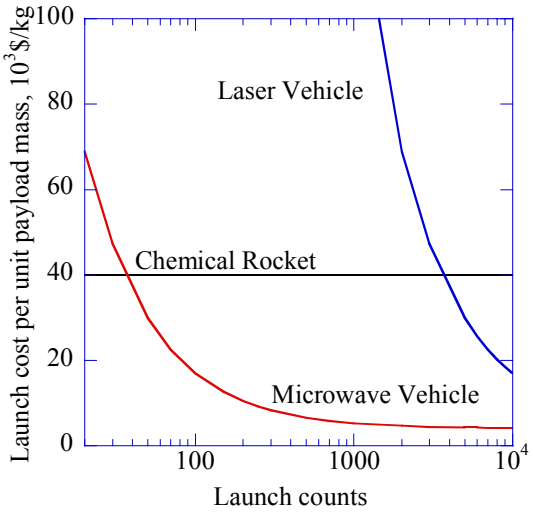

Fig. 16 Launch cost.

SUMMARY

The beam power of 1.6MW per unit initial vehicle mass is optimum to reach GTO trajectory, and 4,000 launches are necessary to redeem the cost for laser transmitter facility.

REFERENCES

[1] Myrabo, L.N., "World Record Flights of Beam-Riding Rocket Lightcraft: Demonstration of "Disruptive" Propulsion Technology," AIAA Paper 01-3798, 2001.

[2] Schall, W.O., Bohn, W.L., Echkel, H.A., Mayerhofer, W., Riede, W., and Zeyfang, E., "Lightcraft Experiments in Germany," *Proc. of the SPIE: High-Power Laser Ablation III*, Vol. 4065, edited by C.R. Phipps, International Society for Optical Engineering, Bellingham, WA, 2000, pp.472-481.

[3] Wang, T-S., Chen, Y-S., Myrabo, L.N. and Mead, F.B.Jr., "Advanced Performance Modeling of Experimental Laser Lightcraft," *J. of Propulsion and Power*, Vol.18, pp.1129-1138, 2002

[4] Katsurayama, H., Komurasaki, K., Momozawa, A. and Arakawa, Y., "Numerical and Engine Cycle Analyses of a Pulse Laser Ramjet Vehicle," *Transactions of JSASS, Space Technology Japan*, Vol.1, pp.9-16, 2003.

[5] Nakagawa, T., Ohmura, S, Komurasaki, K., Arakawa, Y., "Beam quality of phased array lasers for long distance transmission," AIAA-2003-5914, Norfork, VA, 2003.

[6] Mori, K., Komurasaki, K., and Arakawa, Y., "Nozzle scale optimum for the impulse generation in a laser pulsejet." *J. of Spacecraft and Rockets,* to appear.

[7] Mori, K., Hirooka, Y., Katsurayama, H., Komurasaki, K., Arakawa, Y., "Effect of the Refilling Processes on the Thrust Generation of a Laser Pulsejet," *Proc. of 2nd International Symposium on Beamed Energy Propulsion*, edited by K. Komurasaki, American Institute of Physics, Sendai, Japan, Oct. 2003, pp.40-48.

[8] Mori, K., Komurasaki, K., and Arakawa, Y., "Energy transfer from a laser pulse to a blast wave in reduced-pressure air atmospheres," *J. of Applied Physics*, Vol. 95, No. 11, (2004) pp. 5979–5983.

[9] Shiramizu, M., NAL TM 598, 1989 (in Japanese).

[10] Nakagawa, T., Mihara, Y., Komurasaki, K., Takahashi, K., Sakamoto K., Imai, T., "Propulsive Impulse Measurement of a Microwave-Boosted Vehicle in the Atmosphere," *J. of Spacecraft and Rockets*, Vol. 41, No. 1 (2004), pp.151-153.

[11] Oda, Y., Nakagawa, T., Komurasaki, K., Takahashi, K., Kasugai, A., Sakamoto K., Imai, T., "An Observation of Plasma Inside of Microwave Boosted Thruster," *Proc. of 2nd International Symposium on Beamed Energy Propulsion*, edited by K. Komurasaki, American Institute of Physics, Sendai, Japan, Oct. 2003, pp.399-406.